

Lawrence Berkeley National Laboratory

Lawrence Berkeley National Laboratory

Title

DETECTOR MATERIALS: GERMANIUM AND SILICON

Permalink

<https://escholarship.org/uc/item/2tk2b1j4>

Author

Haller, E.E.

Publication Date

1981-11-01

LBL--13898

DE83 001968

DETECTOR MATERIALS: GERMANIUM AND SILICON*

E. E. Haller

Lawrence Berkeley Laboratory and
Department of Materials Science and Mineral Engineering
University of California
Berkeley, California 94720 U.S.A.

DISCLAIMER

This report was prepared as an account of work sponsored by an agency of the United States Government. Neither the United States Government nor any agency thereof, nor any of their employees, makes any warranty, express or implied, or assumes any legal liability or responsibility for the accuracy, completeness, or usefulness of any information, apparatus, product, or process disclosed, or represents that its use would not infringe privately owned rights. Reference herein to any specific commercial product, process, or service by trade name, trademark, manufacturer, or otherwise, does not necessarily constitute or imply its endorsement, recommendation, or favoring by the United States Government or any agency thereof. The views and opinions of authors expressed herein do not necessarily state or reflect those of the United States Government or any agency thereof.

NOTICE

**PORTIONS OF THIS REPORT ARE ILLEGIBLE. It
has been reproduced from the best available**

**November 1981 copy to permit the broadest possible avail-
ability.**

*This work was supported by the Director's Office of Energy Research,
Office of Health and Environmental Research, Pollutant Characterization
and Safety Research Division of the U.S. Department of Energy under
Contract No. DE-AC03-76SF00098.

E. E. Haller
Lawrence Berkeley Laboratory and
Department of Materials Science and Mineral Engineering
University of California
Berkeley, California 94720 U.S.A.

Abstract

This article is a summary of a short course lecture given in conjunction with the 1981 Nuclear Science Symposium. The basic physical properties of elemental semiconductors are reviewed. The interaction of energetic radiation with matter is discussed in order to develop a feeling for the appropriate semiconductor detector dimensions. The extremely low net dopant concentrations which are required are derived directly from the detector dimensions. A survey of the more recent techniques which have been developed for the analysis of detector grade semiconductor single crystals is presented.

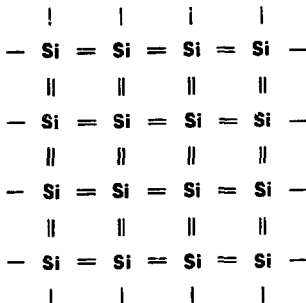
Introduction

Semiconductor nuclear radiation detectors can look back over a more than forty-year-long history. By now they have demonstrated their unique properties in a large number of fields and new exciting applications are reported every year. Much effort and great interest is devoted at the present time to the question: "Can semiconductor detectors be used in large numbers in high-energy physics?" The payoffs of such an application of semiconductors can be drastically demonstrated (and therefore also a little oversimplified) with the possibility of the replacement of a detector like the time-projection chamber (TPC) which is a cylinder, 2m long and 1m in diameter, with a ten times shorter and five to ten times smaller diameter cylinder, fully covered with a large number of two-dimensional silicon array detectors. Such a reduction in volume could be propagated to the large superconducting magnet surrounding TPC and to all the detectors enclosing TPC. With this futuristic outlook we come back to the more modest outline of this particular lecture. The electrical properties of elemental semiconductors which are most important for the radiation detection will be reviewed first. This section is followed by a discussion of nuclear radiation detector dimensions which are dominated by the linear absorption coefficient or the range-energy relation of the various kinds of radiation. The detector dimensions dictate an upper limit of the net impurity concentration which is, compared to the number of germanium or silicon atoms per cm^3 , extremely small. Recently developed techniques for the study of impurities present in such small concentrations are described in some detail. The review closes with a discussion of the progress made in surface passivation.

Elemental Semiconductors

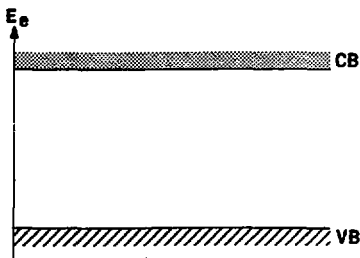
Silicon and Germanium

The properties of the semiconductors Si and Ge which are the most fundamental ones for nuclear radiation detection are what we call the bandgap and net impurity doping. The bandgap is an energy range between the valence band (bound electrons) and the conduction band (free electrons). In this energy range there are no allowed energy values for an electron in a perfect semiconductor (Fig. 1).



A)

B)



PURE CRYSTAL AT T=0 K

NBL 8111-12651

Fig. 1. A pure silicon crystal at T=0 K. The physical information in part A is equivalent to the one in part B. The band schematic in part B is more convenient to indicate electron energies.

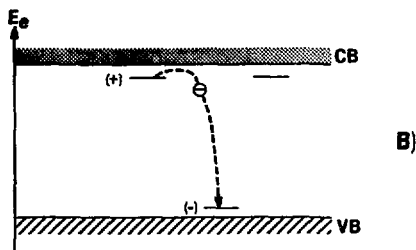
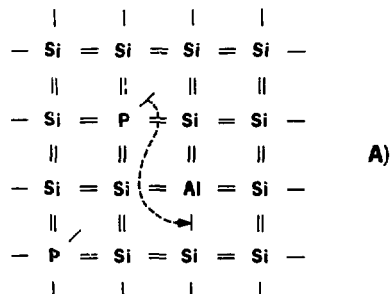
In other terms, this means that we have to transfer at least the bandgap energy to a bound electron in order to break it out of its bond and make it free. This can happen when highly energetic radiation (particles, gamma rays and x-rays) enters a semiconductor crystal. On the other hand, electrons can also be broken out of their bonds by thermal energy (phonons). Every electron which leaves its valence position will leave behind a hole. This "missing electron" or hole can be modeled as a "positive electron". The number of electrons and holes created in this way by radiation or thermal energy (i.e. phonons) must therefore be equal. The thermally generated electrons and holes

lead to the so-called intrinsic carrier concentration n_i :

$$n_i = \sqrt{N_C N_V} \exp(-E_g/2kT) \quad (1)$$

N_C —effective density of states in the conduction band, N_V —effective density of states in the valence band, E_g —bandgap energy (Si: 1.1eV, Ge: .7eV), k —Boltzmann's constant $= 8.65 \times 10^{-5}$ eV/K, T —absolute temperature (K). The intrinsic carriers are dictating the lower limit of the leakage current in a reverse biased diode. This is the fundamental reason for the cooling of germanium detectors (in this respect, there is no difference between gallium-doped, lithium-compensated Ge or high-purity Ge!) and also of very high resolution silicon x-ray detectors. Much effort has gone into producing detectors from semiconductors with a larger bandgap and therefore lower leakage current at room temperature. One of the following lectures discusses the results which have been achieved with HgI₂.

The second property which has been mentioned is related to net impurity doping. The introduction of elemental impurities of the third and fifth group of the periodic table of isotopes makes an elemental semiconductor conduct much more strongly than one would expect from the intrinsic carrier concentration. Of the five valence electrons of a phosphorus atom only four are needed to complete the bonds to the four Si or Ge neighbors. The fifth electron is very loosely bound, actually with about one fortieth to one sixtieth of the bandgap energy. Because it is so weakly bound, it takes very little thermal energy to free such a carrier into the valence band. This situation is described in the band schematic by a so-called "state" close to the conduction band (Fig. 2). A short line, a few meV below the conduction band, shows that there is an energetically permitted place for one electron. In close analogy, one describes the hole which is created when an aluminum impurity atom binds a fourth electron which comes from somewhere in the valence band. It again takes very little energy to move a valence electron from a valence band place into a group three impurity place. The hole which is created can move freely through the crystal and it acts like a positive electron. Following this simple picture one calls group III impurities acceptors and group V impurities donors. When both donors and acceptors are present in a crystal (which is true in all real crystals) the donor electrons can fall into acceptor levels (Fig. 2). Energetically this is preferred over the emission into the conduction band. Neither the donor nor the acceptor produce now a free carrier i.e., the two compensate each other.



P & Al DOPED CRYSTAL AT T=0 K

xs: 8111-1269C

Fig. 2. Introduction of group III and V impurities (Al, P) leads to energy levels in the bandgap.

This is the mechanism which explains why we only care about the net impurity concentration, either $N_A - N_D$ for $N_A > N_D$ or $N_D - N_A$ for $N_D > N_A$.

It has been stated above that it takes little but not zero energy to free a bound phosphorus electron to the conduction band. When a germanium crystal is cooled to low temperatures, we find that the thermal energy becomes too small for the ionization of a donor at around 15 to 20K. In silicon crystals, the "freeze out" or ceionization occurs already at around 60-70K. The actual freeze-out temperature depends on both the concentration of donors and acceptors. This freeze out of the free carriers explains why one has to expect a possible change in the operational characteristics of semiconductor radiation detectors used at very low temperatures (e.g. liquid helium temperature 4.2K). At such low temperatures, the compensated fraction of donors and acceptors which do not freeze out can act as efficient charge traps. A high enough reverse bias diminishes the trapping action substantially, and fully depleted high-purity germanium detectors have successfully been used at around 4K. A more quantitative description for the emission rate of an electron from a donor or a hole from an acceptor is obtained with the following equation:

$$e = \langle v \rangle n_{\text{band}} \exp(-E/kT) \quad (2)$$

with e —carrier emission rate (s^{-1}); $\langle v \rangle$ —average thermal velocity (cm s^{-1}) $= (3kT/m^*)^{1/2}$; n_{band} —effective density of states (cm^{-3}) $= 2(2\pi m^* kT/h^2)^{3/2}$; E —binding energy of an electron ($E_C - E_D$) or a hole ($E_A - E_V$); $E = 0$ meV for Ge and $E = 40$ meV for Si; and $k = 8.65 \times 10^{-5}$ eV/K. The above equation is valid not only for the group V and group III impurity levels but also for "deep" impurity levels caused by a large variety of elemental impurities and impurity complexes. The emission rate for any given level is very important for the time allotted to the charge collection in a radiation detector. So long as $e^{-\tau} \ll \tau$, the dominant or overall filter rise time or peaking time, we do not have to consider charge losses due to trapping. When $e^{-\tau} \sim \tau$, we expect incomplete charge collection within the given time. We recognize that trapping depends very strongly on the position of an energy level and on the detector operating temperature. Experience with some silicon

detectors demonstrates this dependence very effectively. While many silicon crystals can be used to fabricate good room temperature detectors, several of these detectors show severe trapping when cooled to liquid nitrogen temperature (77K). The latter detectors obviously contain traps which are effective at 77K but not at 300K.

So far most of the discussion has been focused on the sources of free electrons and holes and on their interaction with impurity levels. Carrier transport in an electric field is the last phenomenon to be described before coming to the actual semiconductor detectors. At low electric fields the drift velocity \bar{v} is proportional to the E field:

$$\bar{v} = \mu E^2 \quad (3)$$

The proportionality constant is called mobility μ . Typical values for μ are (all values in cm^2/Vs):

		300 K	77 K
Ge	μ_e	3.9×10^3	4.0×10^4
	μ_h	2.3×10^3	4.0×10^4
Si	μ_e	1.9×10^3	1.9×10^4
	μ_h	4.3×10^2	8.0×10^3

At high electric fields the drift velocity becomes comparable with the average thermal velocity. The electrons or holes become "hot" and equation (3) becomes invalid. In the high field limit, the carriers generate phonons (lattice vibrations) and lose energy at a rate equal to the energy gained in the E field. The drift velocity saturates at around 10^7 cm/s . This value is, interestingly enough, very similar for most semiconductors. This fact has an important significance which is quite often overlooked. Semiconductors which have a low intrinsic mobility (not lowered by deep traps) may be biased at high fields which can bring the carriers close to saturation velocity. This means that a large difference in mobility does not necessarily lead to similarly large differences in signal rise times.

Semiconductor Nuclear Radiation Detectors: Interaction with Energetic Radiation and Detector Dimensions

The basic structure of a planar detector $n^+ - i - p^+$ diode is shown in Fig. 3.

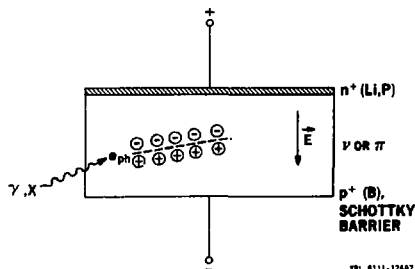


Fig. 3. Schematic cross section of a planar $n^+ - i - p^+$ radiation detector diode.

Contacts of opposite type sandwich a low impurity concentration n or p (γ or x) region. Signal formation for x - and γ -rays can evolve through the following stages: The high energy photon interacts with a K-shell electron (or with higher shells but with much lower probability) and gives up all of its energy to this electron. This full energy photon conversion is called photoeffect. The kinetic electron energy is $E_{\text{photon}} - E_{\text{shell}}$, an energy which is usually much larger than the bandgap. Through interactions with valence electrons, a large number N of electron-hole pairs are created. In the E -field of the detector, produced by the applied reverse bias, the electrons and holes separate and drift to the contacts. The x -rays produced during the filling of the K, L, etc. shells produce further photoelectrons which generate additional electron-hole pairs. After all the free carriers have been collected at the contacts, one observes a charge Q which is proportional to the energy of the incident photon. One has found experimentally:

$$N = E_{\text{photon}}(eV) / \epsilon \quad (4)$$

with $\epsilon_{\text{Ge}} = 3.0 \text{ eV}$ and $\epsilon_{\text{Si}} = 3.8 \text{ eV}$. The fluctuation of N is ΔN :

$$\Delta N = \sqrt{F N} \quad (5)$$

$F=0.1$ for Si, Ge. F is called Fano factor. It is <1 in the case of Si and Ge. In gases, Fano factors larger than unity have been observed. The small energy needed to produce an electron-hole pair and the small Fano factor lead to an energy resolution of semiconductor detectors which is substantially better than any other broad band detection scheme (i.e. gas proportional counters, scintillators coupled to photomultipliers, etc.). Fifteen-year-old spectra of gamma rays from neutron activated pottery (Fig. 4) illustrate the superior energy resolution quite drastically although today's NaI scintillators have a somewhat better energy resolution than that shown in Fig. 4.

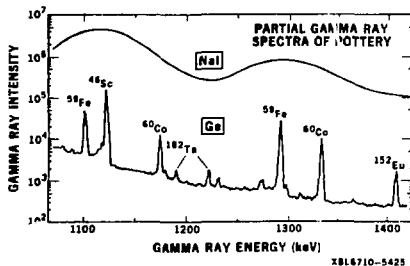


Fig. 4. Spectra of neutron activated pottery recorded with a NaI scintillator and with a germanium detector.

Compton scattering, the classical billiard ball type scattering of photons off electrons and pair production for photon energies $E_{\text{photon}} > 2m_0c^2$ (1022 keV) are two further interaction processes of photons and the silicon or germanium crystal. Because all of these processes are statistical in nature, we can write for the number of interactions dI per length of semiconductor crystal dx :

$$dI = -\alpha_L I dx \quad (6)$$

with α_L = linear absorption coefficient (cm^{-1}) and

$I = \text{photon flux}$. We ignore here all secondary or higher order interaction sequences such as a Compton event followed by a photo effect, etc. These higher order events lead to larger number of full energy conversion (or photo peak) events. The reader may figure out for him/herself what happens when one lets the detector size grow to infinity! The total linear absorption coefficients for Si and Ge are plotted in Figs. 5 and 6 respectively.

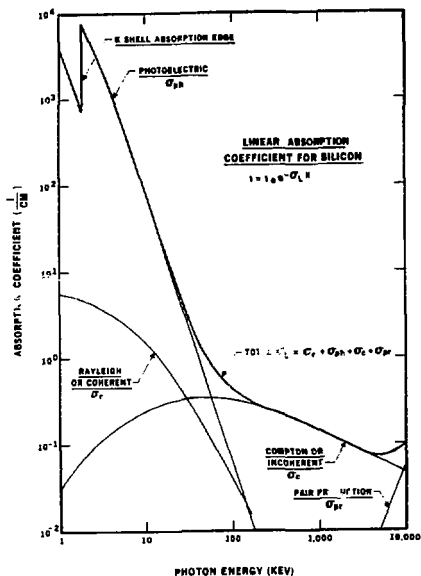


Fig. 5. Linear absorption coefficient of photons (gamma and x-rays) for Si.

Integration of the differential absorption equation leads to the exponential equation shown in the figures. The strong energy and atomic charge dependences of photoelectric are clearly shown in the two plots. Above 200keV the total absorption coefficient is not very different for Si and Ge. The total fraction of photons absorbed by two thicknesses of Si and Ge is shown in Fig. 7. The well known fact that Ge detectors have to be used above ~40keV is apparent.

Electrons and ions interact directly with the lattice nuclei and electrons. There is no statistical conversion process necessary before ionization (i.e. electron-hole pair production) can take place. The range-energy concept is applicable in these cases. The range-energy relationships for a number of ions are plotted in Fig. 8 for Si and in Fig. 9 for Ge.

This brief overview of the absorption of photons and the stopping of ions and electrons shows that semiconductor detectors with a total active thickness from a few μm up to 10cm are required for the measurement of nuclear radiation extending over a typical energy range from hundreds of eV to over 100MeV. An

active thickness above a couple of centimeters is obtained with stacks of individual detectors called detector telescopes.

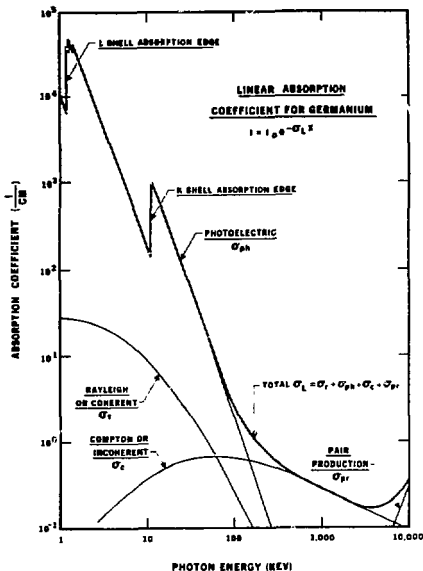


Fig. 6. Linear absorption coefficient of photons for Ge.

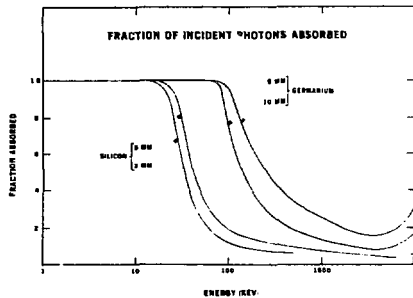


Fig. 7. Fraction of absorbed photons in Si and Ge.

Using Fig. 3 we have discussed the planar, reverse biased semiconductor detector. What are the limitations on the physical size of such a detector? The physical parameter of utmost importance for large detectors is the net impurity concentration. Crystals of over 30cm diameter and tens of cm long have been grown for optical applications. The necessarily

low $|N_A - N_D|$, however, is very difficult to obtain. The net acceptor or donor concentration represents a space charge in a reverse biased diode.

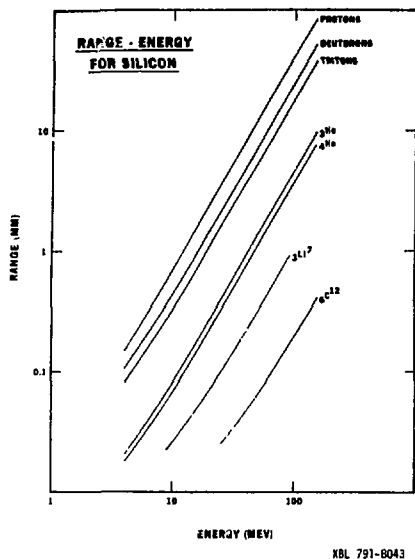


Fig. 8. Range-energy relation for ions in Si.

Poisson's equation relates the electric potential ϕ to the space charge:

$$\Delta\phi = -e|N_A - N_D| / \epsilon_0 \epsilon_0 \quad (7)$$

with e -charge of the electron $= 1.6 \times 10^{-19} \text{As}$; ϵ_0 - permittivity of vacuum $= 8.85 \times 10^{-12} \text{As/Vm}$; ϵ_0 - relative dielectric constant; $\epsilon_{Si} = 11.7$, $\epsilon_{Ge} = 16.0$. For a planar diode, we can solve the above equation in one dimension and obtain:

$$\phi = w^2 |N_A - N_D| e / 2\epsilon_0 \quad (8)$$

with w - width of the depletion layer. Using the known values for e , ϵ_0 and ϵ_0 , we obtain for Si:

$$\phi_{Si} = 7.72 \times 10^{-8} (\text{Vcm}) w^2 (\text{cm}^2) |N_A - N_D| (\text{cm}^{-3}) \quad (9)$$

and for Ge:

$$\phi_{Ge} = 5.64 \times 10^{-8} (\text{Vcm}) w^2 (\text{cm}^2) |N_A - N_D| (\text{cm}^{-3}) \quad (10)$$

We can figure out that it takes 1128V to deplete a 1cm thick Ge diode with a net impurity concentration of $2 \times 10^{10} \text{cm}^{-3}$. Up to several thousand volts can be called reasonable biases for radiation detector diodes. This in turn means that $|N_A - N_D|$ must be of the order of a few times 10^{10}cm^{-3} , an extremely small relative net impurity concentration (compare to $4 \times 10^{22} \text{Ge cm}^{-3}$). With Pell's invention of the Li-compensation technique—using the drifting of lithium ions in an electric field—it became feasible to reach the necessary low net concentrations.² About ten years ago

the first successful attempts at growing ultra-pure Ge crystals with $|N_A - N_D| = 10^{10} \text{cm}^{-3}$ were reported by R. N. Hall et al.³ and W. L. Hansen et al.⁴ This advance made detector fabrication more predictable and also easier. It is no exaggeration when detector makers claim that a simple planar p-n Ge diode can be produced and tested in one day provided that the Ge crystal is of good quality. With the exception of extremely large coaxial Ge detectors, all Ge nuclear radiation detectors are made from ultra-pure germanium. This overwhelming success should not lead to the assumption that the production of ultra-pure germanium is easy and that it has become a routine operation. Quite the opposite is true and substantial work is still required to understand and control the purification and crystal growth of ultra-pure germanium.⁵

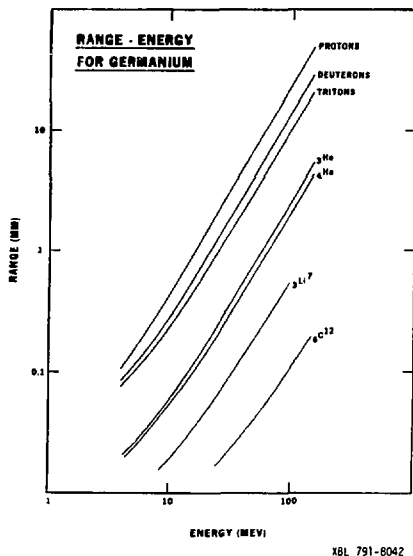


Fig. 9. Range-energy relation for ions in Ge.

Measurement of Impurity Levels: Concentration and Species

After having discussed the net impurity concentrations which are required in the extreme case of large volume gamma ray detectors (detectors with smaller depletion width obviously are less demanding on the impurity concentration), we return in this section to the nature of impurity levels, to the measurement of their concentration and to the determination of their specie(s). Let us first divide the impurity levels into two categories: shallow levels and deep levels. Shallow levels do not trap free charges for long enough times at typical detector operating temperatures to have any detrimental effects on the charge collection. Shallow levels are produced by the group III and the group V elements and also by lithium. The ionized shallow levels contribute space charge leading to the finite depletion layer for a given reverse bias.

Ionized deep levels also contribute space charge in a reverse biased diode. The detrimental effect of deep levels is the trapping of free charge carriers. Deep levels have to be eliminated from high quality detector crystals.

The shallow net impurity concentration of silicon single crystals can be measured at room temperature. It is typically derived from a resistivity measurement (ρ) using the following equation:

$$\rho = \frac{1}{e\mu(N_A - N_D)} \quad (11)$$

with μ =mobility, $\mu_e(300K)=1900\text{cm}^2/\text{Vs}$, $\mu_h(300K)=430\text{cm}^2/\text{Vs}$; e =charge of the electron= $1.6 \times 10^{-19}\text{As}$; $|N_A - N_D|$ =net impurity concentration. Resistivity measurements can be made accurately and reliably up to $\sim 50\text{k}\Omega\text{cm}$. Above this value it becomes very difficult to obtain precise data. The intrinsic resistivity of silicon at room temperature is $220\text{k}\Omega\text{cm}$ and has been derived from measurements made at higher temperatures.

The intrinsic carrier concentration of germanium at room temperature is $3.5 \times 10^{13}\text{cm}^{-3}$ which yields a resistivity of $50\Omega\text{cm}$. Ultra-pure germanium exhibits substantially lower impurity concentrations and it has to be cooled, most conveniently to liquid nitrogen temperature (77K), in order to reduce the intrinsic carrier concentration to low enough values. A simple resistivity measurement or a Hall effect measurement leads to the net impurity concentration.

It is not necessary for the detector user or manufacturer to know exactly which elemental impurities create the shallow acceptor and donor levels in a particular crystal. The person who deals with purification and crystal growth, however, depends strongly on this information. Because the technique which yields the impurity species is, in principle, simple and elegant and because it has led to the discovery of a large number of unknown acceptor and donor species, we will devote some space to a brief description. The technique is based on the fact that shallow impurity levels in semiconductors show several analogies to a hydrogen atom. A phosphorus donor, for example, can be modeled with a fixed positive charge, the phosphorus ion, binding an electron in its Coulomb field. Such a "hydrogenic" donor has, besides its ground-state, several excited states just as in the hydrogen atom. Table 1 contains the relevant equations and some values for the binding energy and the Bohr radius of hydrogen and of shallow levels in Ge. The major difference lies in the reduction of the energy by the square of the dielectric constant of Ge ($\epsilon_r=16$) and by the reduced mass of the electron $m^* = 0.3m_0$. The Bohr radius, on the other hand, increases linearly with ϵ and with $(m^*)^{-1}$. Infrared absorption measurements on doped Si and Ge crystals showed in the late 1950's that a series of excited states do exist for all known shallow donors and acceptors. Absorption spectroscopy is quite insensitive at least on the scale of impurity concentrations discussed in the present context. The combination of IR-spectroscopy with photoconductivity overcomes the sensitivity problem. Lifshits and Nad⁶ were the first to use this so-called photothermal ionization spectroscopy. Figure 10 illustrates the principle of the technique. IR photons can excite the electron residing in the groundstate of a donor to a bound excited state only if they have precisely the energy corresponding to the energy difference between the two states. Once the electron resides in a bound excited state it can absorb, with a certain probability, a phonon which can lift it into

the conduction band where it represents a free carrier. The measurement of the conductivity in function of the photon energy (or typically wave-number $\nu \times 10^{-1}$ in cm^{-1} , $8.065\text{cm}^{-1} = 1\text{meV}$) yields a series of sharp peaks at all the energies which lead to a transition from the groundstate to a bound excited state. A section of a spectrum obtained with an ultra-pure Ge crystal containing the residual acceptor aluminum is shown in Fig. 11.

HYDROGEN

$E = -\frac{e^4 m}{2\hbar^2}$
$r = \frac{\hbar^2}{e^2 m}$
H { 13.6eV ~5Å

SEMICONDUCTOR (ACCEPTOR OR DONOR)

$-\frac{e^4 m^*}{2\epsilon^2 \hbar^2}$
$\frac{\epsilon \hbar^2}{e^2 m^*}$
Ge { 6meV 80Å



- VERY SMALL BINDING ENERGIES
- VERY LARGE ORBITS SPREADING OVER THOUSANDS OF UNIT CELLS

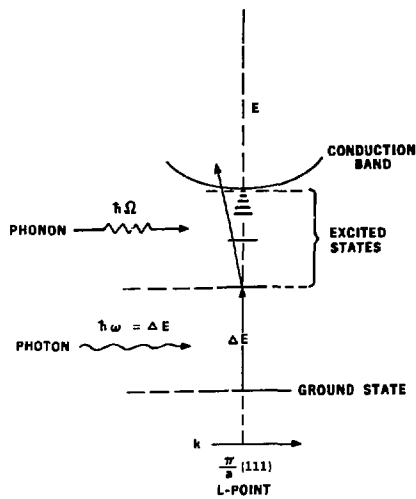
XBL 6111-11665

Table 1.

Photothermal Ionization Spectroscopy (PTIS) combines several advantageous features: a) The sensitivity does not depend in first order on the impurity concentration because both the "dark" conductivity and the conductivity increase with light depend linearly on the net impurity concentration. b) The purer the crystal is, the higher the resolution will be. This is true to about a net concentration of 10^{11}cm^{-3} . At such low concentrations, virtually all the impurities are spatially separated so far that no overlapping of wave functions (one cause of line broadening) occurs. c) The excellent energy resolution allows the separation of all the known acceptors and donors and has led to the discovery of several new centers.

The extensive application of PTIS⁵ has guided the development of ultra-pure germanium and has led to some understanding of the impurity chemistry. One of the surprising findings was the nonsegregating behavior of aluminum in crystals grown from a melt contained in a quartz crucible. Another surprise was the discovery of acceptor and donor centers which appear to be composed of two or more impurities which may be neutral by themselves. One such center is sketched in Fig. 12. A silicon impurity in germanium traps a hydrogen atom in its strain field. The hydrogen atom can complete its 1s shell by accepting a second electron from the germanium valence band. By accepting an electron, the center becomes an acceptor called A(H,Si). A similar center with carbon in place of silicon has been found. Figure 13 shows the well-

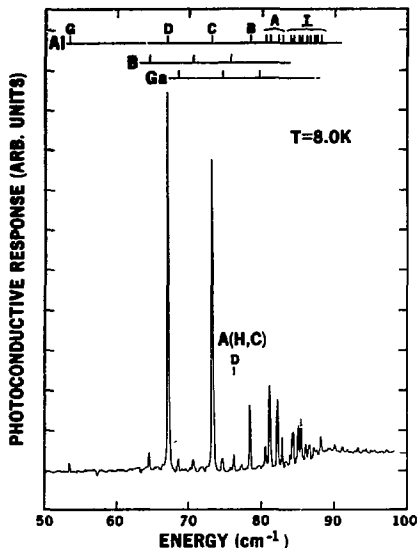
known D(H₂O) or "rapid quench donor" as R. N. Hall called this center.



NBL 7411-8629

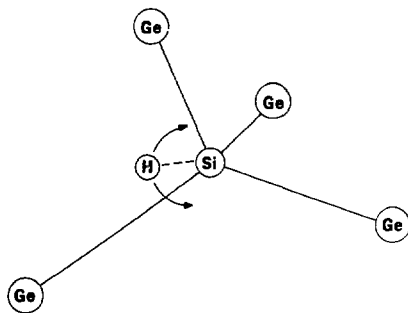
Fig. 10. Photon absorption followed by phonon absorption leads to ionization of a shallow donor.

The next measurement technique to be discussed has been developed specifically for deep levels.⁷ It is a parametric technique based on the capacitance measurement of a reverse biased diode. It can be directly applied to nuclear radiation detectors provided that a variable temperature cryostat is available. Deep Level Transient Spectroscopy (DLTS) uses the fact that the emission rate of an electron or hole from a deep donor or deep acceptor is an exponential function of the temperature and the level binding energy. When the reverse bias is repetitively pulsed between two values, a volume between these two depletion widths is filled and emptied of free carriers (Fig. 14). Shallow levels will follow the bias changes very rapidly down to low temperatures. Deep centers will give up their charge with a specific time constant τ (see Equation 2). The charge state situation is directly reflected in the total space charge and in the capacitance. The bias and capacitance relation is displayed for a hypothetical trap in Fig. 15. In order to obtain a spectrum, one uses an electronic "filter" which produces a maximum output for a given, variable time constant. Emission "rate window" is the expression which has been adopted for such a filter. Lock-in amplifiers, boxcar integrators and for the best signal-to-noise ratio, a correlator are used to realize a "rate window". Figure 16 shows a block schematic of a correlator setup. The reverse biased diode is kept in a variable temperature cryostat. The capacitance is measured with any common capacitance bridge. The capacitance signal is processed in the correlator which produces a maximum output for a selectable time constant between 1 and 100ms in this particular case. Keeping the time constant fixed at a given value and changing the temperature from room temperature down to a few degrees K



HEL 876 174

Fig. 11. Typical residual aluminum spectrum obtained with a small Ge sample.



HEL 106-11222

Fig. 12. The tunneling hydrogen model for the acceptor A(H,Si) in pure Ge.

produces a DLT spectrum. Every deep level will have its emission rate or its inverse—the emission time constant—equal to the correlator time constant at a specific temperature. Above this temperature the time constant for emission will be too short to be picked out by the correlator and below that temperature the time constant will be too long. Figure 17 shows a Deep Level Transient Spectrum of an ultra-pure germanium p⁺-n⁺ diode containing copper and copper-hydrogen acceptors.⁷ The copper acceptor can bind up to three holes leading to three levels in the bandgap.

One of these levels is located in the upper half of the bandgap. This means that the third hole cannot be ionized in p-type germanium at any temperature. It therefore does not lead to a peak in the spectrum. The strongly nonlinear temperature axis is caused by the nonlinear response of the Si diode temperature sensor. The same spectrum is displayed in Fig. 18 with a linearized temperature axis.

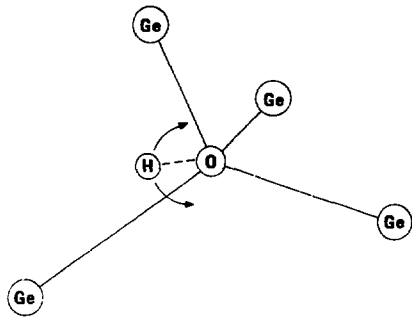


Fig. 13. Schematic of the hydrogen-related donor D(H, O) in Ge.

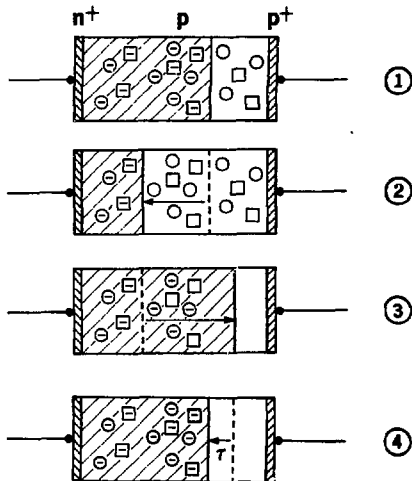


Fig. 14. Charge states in a p^+-n^+ diode under various reverse biasing conditions.

DLTS has turned out to be a very powerful technique to detect and to study deep levels in nuclear radiation detectors. Besides the deep levels which are due to impurities or impurity complexes, one can study deep levels due to dislocations and radiation

defects. As a guideline for the sensitivity of DLTS, one can assume that deep level concentrations 10^4 times smaller than the net impurity concentration can be detected. This superb sensitivity can often be a problem because too many peaks appear, some of which are due to surface states and other artifacts.

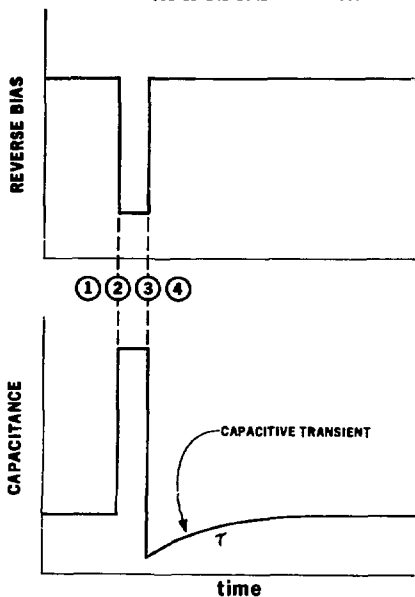


Fig. 15. Bias and capacity sequence as a function of time in a typical DLTS measurement.

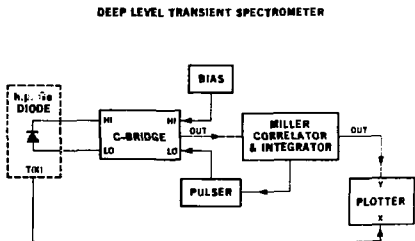


Fig. 16. Block schematic of a DLTS setup using a correlator.

A further analytical tool used for the study of neutral impurities is based on the very old radioactive tracer technique. The novel idea is the use of the excellent semiconductor detector properties to

measure internally the radiation emitted by the radio tracer. This idea has been applied for the first time to the study of carbon in germanium.⁸

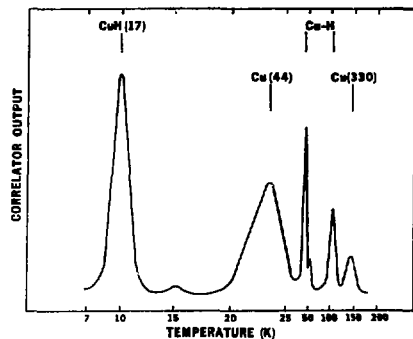


Fig. 17. DLT spectrum of a p^+-n^- Ge diode containing copper and copper-hydrogen acceptors.

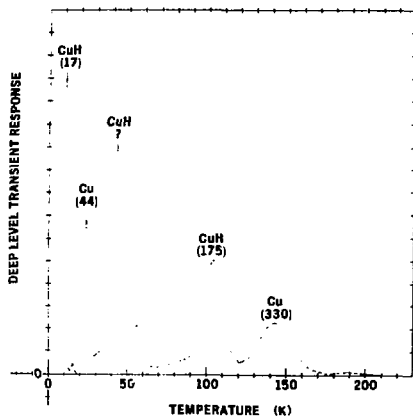


Fig. 18. Same spectrum as in Fig. 17 but with linearized temperature axis.

The availability and the long half life of ^{14}C make it easy to incorporate this isotope into a germanium single crystal by growing it from a crucible coated with ^{14}C -spiked graphite. The sensitivity of the method is mainly limited by the radiation from the surroundings of the detectors. In a low background environment (six counts per minute in the 10 to 160keV interval) we have estimated that with a 10% ^{14}C carbon fraction, one can detect 10^8 carbon atoms cm^{-3} with a three sigma accuracy. In this experiment, the concentration of carbon turned out to be so large ($[\text{C}] = 10^{14} \text{cm}^{-3}$) that the ^{14}C -beta spectrum shape could be measured accurately. An active guard ring detector (Fig. 19) was used in order to suppress surface effects. Figure 20 shows the

actual beta spectrum. The agreement between the experimental data and the predicted spectrum shape for allowed beta decay (solid line) is excellent. A Fermi-Kurie plot makes it easier to check the agreement (Fig. 21).

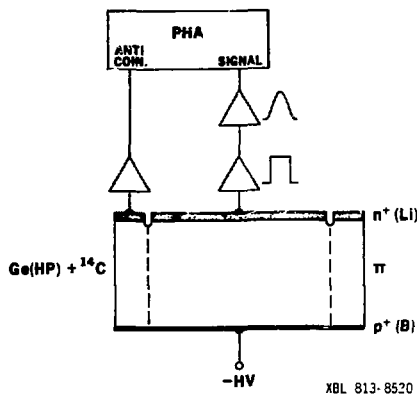


Fig. 19. Active guard ring detector used for the internal detection of betas from ^{14}C decays.

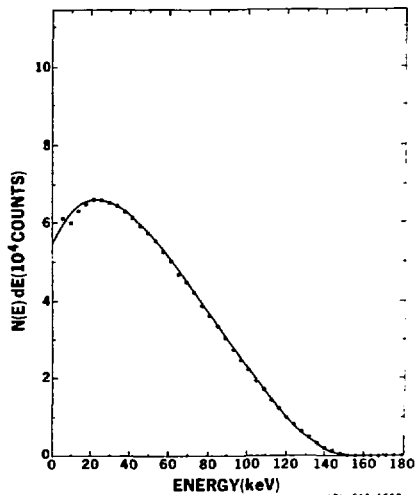


Fig. 20. The energy spectrum of betas from ^{14}C decays (dots). The continuous line is the spectral shape predicted for an allowed transition.

Acknowledgements

Many colleagues have contributed to the material reviewed in this lecture. The limited space permits mention of only a few names: Leo M. Falicov, Fred S. Goulding, William L. Hansen, G. Scott Hubbard, Paul N. Luke, Paul L. Richards and John T. Walton.

This work was supported by the Director's Office of Energy Research, Office of Health and Environmental Research, Pollutant Characterization and Safety Research Division of the U.S. Department of Energy under Contract No. W-7405-ENG-48.

References

1. See for example: Kittel C, "Introduction to Solid State Physics", any ed., Wiley Interscience, ch. on semiconductors; and Smith R P, "Semiconductors", 2nd ed., Cambridge University Press (1978).
2. Pell E W, J. Appl. Phys. 31, 291 (1960).
3. Hall R N and Soltys T J, IEEE Trans. Nucl. Sci. NS-18, 160 (1971).
4. Hansen W L, Nucl. Instr. Meth. 94, 377 (1971).
5. See for example: Haller E E, Hansen W L and Goulding F S, Adv. Phys. 30, 93 (1981).
6. For a recent review see: Kogan Sh. M. and Lifshits T M, Phys. Stat. Sol. (a) 29, 11 (1977).
7. For an application of DLTS to pure germanium see: Haller E E, Li P P, Hubbard G S and Hansen W L, IEEE Trans. Nucl. Sci. NS-26, 265 (1979).
8. Haller E E, Hansen W L, Luke P, McMurray R E Jr. and Jarrett B, IEEE Trans. Nucl. Sci. NS-29, No. 1 (1982) in print.
9. Hansen W L, Haller E E and Hubbard G S, IEEE Trans. Nucl. Sci. NS-27, 247 (1980).

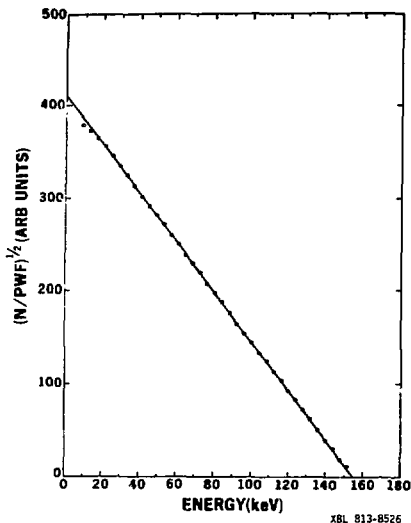


Fig. 21. The Fermi-Kurie plot of the data displayed in Fig. 20. This kind of plot makes it easy to check deviations of the data from the theory.

Detector Surfaces

This section is devoted to the recent progress which has been made in passivating the bare surfaces of large volume germanium gamma-ray detectors. In a perfect planar p^+i-n^+ detector (Fig. 3), the electric field lines will be perpendicular to the n^+ and p^+ electrodes and parallel to the bare surface throughout the whole volume. The deposition of a few charges (ions) on the bare surface will lead to a distortion of this electric field pattern. Because the net impurity concentration in the Ge bulk is very low, it takes very few charges to produce strong field distortions or surface channels. Such channels are usually undesirable because they lead to incomplete charge collection near the bare surfaces. Numerous schemes have been tried to avoid the surface channel. The use of a guard ring is a solution. The reduction in active detector volume, however, may be unacceptable. Chemical surface treatment and evaporated films have been used to reduce the surface charge. More recently a technique has been developed by Hansen et al⁹ which seems to fulfill all the requirements for a perfect surface passivation. A hydrogenated amorphous germanium film is deposited by RF sputtering on the bare surfaces of a finished detector. The hydrogen concentration in the sputtering gas (argon) can be matched to the bulk net impurity concentration so as to lead to a perfectly neutral surface. The deposited film does not increase the noise in the device and it protects detectors from moderate contaminations. The experience with a large number of high-energy ion detector telescopes (stacks of detectors) over the last three years has been very good. None of the detectors seems to have become inoperative because of surface contamination even though many of the devices have been annealed numerous times to remove radiation damage.